



Published in final edited form as:

Placenta. 2020 April ; 93: 113–118. doi:10.1016/j.placenta.2020.03.004.

EXPLORING IN VIVO PLACENTAL MICROSTRUCTURE IN HEALTHY AND GROWTH-RESTRICTED PREGNANCIES THROUGH DIFFUSION-WEIGHTED MAGNETIC RESONANCE IMAGING

Nickie ANDESCAVAGE, MD^{1,4}, Wonsang YOU, PhD², Marni JACOBS, PhD^{3,4}, Kushal KAPSE, MS², Jessica QUISTORFF, MPH², Dorothy BULAS, MD^{2,5}, Homa AHMADZIA, MD⁶, Alexis GIMOVSKY, MD⁶, Ahmet BASCHAT, MD⁷, Catherine LIMPEROPOULOS, PhD^{2,4,5}

¹Division of Neonatology, Children's National Health System, 111 Michigan Ave. NW, Washington, DC 20010

²Division of Diagnostic Imaging & Radiology, Children's National Health System, 111 Michigan Ave. NW, Washington, DC 20010

³Division of Biostatistics & Study Methodology, Children's National Health System, 111 Michigan Ave. NW, Washington, DC 20010

⁴Department of Pediatrics, George Washington University School of Medicine, 2300 Eye St. NW, Washington, DC 20052

⁵Department of Radiology, George Washington University School of Medicine, 2300 Eye St. NW, Washington, DC 20052

⁶Division of Maternal Fetal Medicine, Department of Obstetrics and Gynecology, George Washington University School of Medicine, 2300 Eye St. NW, Washington, DC 20052

⁷Department of Gynecology and Obstetrics, Johns Hopkins Center for Fetal Therapy, 600 North Wolfe Street, Nelson 228, Baltimore, MD 21287

Abstract

Introduction—Gross and microstructural changes in placental development can influence placental function and adversely impact fetal growth and well-being; however, there is a paucity of in-vivo tools available to reliably interrogate in vivo placental microstructural development. The objective of this study is to characterize in-vivo placental microstructural diffusion and perfusion in healthy and growth-restricted pregnancies (FGR) using non-invasive diffusion-weighted imaging (DWI).

Corresponding Author: Catherine Limperopoulos, Ph.D., Children's National Health System, 111 Michigan Ave. NW, Washington, D.C. 20008, climpero@childrensnational.org, Tel: 202-47605293.

Conflicts of Interest: The authors report no conflict of interest

Publisher's Disclaimer: This is a PDF file of an unedited manuscript that has been accepted for publication. As a service to our customers we are providing this early version of the manuscript. The manuscript will undergo copyediting, typesetting, and review of the resulting proof before it is published in its final form. Please note that during the production process errors may be discovered which could affect the content, and all legal disclaimers that apply to the journal pertain.

Methods—We prospectively enrolled healthy pregnant women and women whose pregnancies were complicated by FGR. Each woman underwent DWI-MRI between 18 and 40 weeks gestation. Placental measures of small (D) and large (D^*) scale diffusion and perfusion (f) were estimated using the intra-voxel incoherent motion (IVIM) model.

Results—We studied 137 pregnant women (101 healthy; 36 FGR). D and D^* are increased in late-onset FGR, and the placental perfusion fraction, f , is decreased ($p < 0.05$ for all).

Discussion—Placental DWI revealed microstructural alterations of the in-vivo placenta in FGR, particularly in late-onset FGR. Early and reliable identification of placental pathology *in vivo* may better guide future interventions.

Keywords

Placenta; fetal growth restriction (FGR); magnetic resonance imaging (MRI); diffusion weighted imaging (DWI); intra-voxel incoherent motion analysis (IVIM)

Introduction

Placental insufficiency deprives the developing fetus of essential metabolites necessary for normal growth and brain development, resulting in fetal growth restriction (FGR). FGR remains a leading cause of stillbirth and a major risk factor for premature birth, cerebral palsy and lifelong morbidity (1–3). Despite advances in fetal diagnostic techniques, there are few current clinical tools that directly and noninvasively assess placental function in utero, often presenting late in placental dysfunction (4, 5). Similarly, despite histopathology descriptions of altered placenta development in FGR, there are no current clinical tools to assess in vivo microstructural development of the placenta (6, 7).

Diffusion-weighted magnetic resonance imaging (DW-MRI, or DWI) measures the movement of water molecules in a given space. In the human body, the molecular diffusion of water is impacted by cell membranes, tissue cellularity and the extracellular space, resulting in decreased diffusion across areas of increased tissue cellularity (8). These principles have been used in biomedical imaging to provide clinical insight into local microstructural integrity, without the need for invasive measures or exogenous contrast (8). The intravoxel incoherent motion (IVIM) analysis approach of DWI capitalizes on differences in tissue organization and the vascular system to inform microstructural development, namely tissue cellularity and microcirculation of a given region (9). The primary metrics of IVIM include (a) the diffusion coefficient, D , an estimate of small-scale diffusion, reflective of tissue cellularity, (b) the pseudo-diffusion coefficient, D^* , an estimate of large scale diffusion and microcirculation of regional capillary networks and (c) the perfusion fraction, f , the percent of moving blood volume in a given region.

DWI and IVIM analyses have also been applied to the study of the human placenta, and revealed regional abnormalities in the perfusion fraction in high-risk pregnancies (10–12). However much less is known about changes in placental water diffusion through-out pregnancy, either in healthy or pathologic states. The objective of this study was to delineate the in vivo diffusion properties of the human placenta in pregnancies with established fetal growth restriction (FGR) as well as healthy, uncomplicated pregnancies to explore in vivo

placental microstructure. We hypothesized that placental perfusion fraction and diffusion coefficients would be reduced in FGR compared to healthy controls due to microstructural alterations in the growth-restricted placenta, evidenced by postnatal histopathology that show inflammatory changes in villous development, as well as vascular changes including thrombosis and infarction in early- and late-onset FGR (7, 13). Furthermore, we hypothesized that diffusion properties would differ in distinct sub-groups of FGR, reflecting the pathologic differences in functional and microstructural placental development across high-risk populations (14).

Methods

Subjects

We recruited pregnant women with singleton pregnancies after 18 weeks gestation as part of a longitudinal prospective observational study at Children's National Health Systems (CNHS) which includes up to two detailed fetal-placental evaluations through advanced MRI, neonatal evaluations and long-term follow-up of this cohort through early childhood. This study is designed as a cross-sectional analysis of placental development from the first fetal-placental evaluation using IVIM. A pregnancy was considered complicated by FGR if the estimated fetal weight was < 10th centile from standard sonographic measures (15) and there was no evidence of congenital anomalies or infections; FGR cases were excluded if there was evidence of congenital infections or dysmorphic features. Healthy controls had no significant past medical history, without chronic or pregnancy induced illnesses, including normal screening studies at the time of enrollment. Exclusion criteria for either group included any maternal contraindications to MRI for either group. The study was approved by the hospital's Institutional Review Board and written informed consent was obtained from all participants.

Imaging: MRI acquisition

All women underwent the same MRI imaging protocol on a 1.5T Discovery MR450 scanner (GE Healthcare, Milwaukee, Wisconsin) using an 8-channel cardiac array (receive only) coil (USAI, Aurora, OH). Pregnant women were positioned in the left lateral or supine position, based on maternal preference for their comfort. The coil array was positioned covering the entire abdomen and pelvis to improve spatial resolution.

Dedicated anatomic single shot fast spin echo (SSFSE) fat suppressed T2-weighted images were acquired in the maternal axial or coronal plane for full placental coverage (TE=160ms, TR=1100ms, 4mm slice thickness). Pulsed gradient spin echo (PGSE) sequences were acquired (TE =53.8 ms, TR=8000 ms, data matrix size 96×96, field of view (FOV) 420×420mm², 4mm slice thickness) with the following b-values: 0, 25, 50, 114, 243, 500, 543, 800, 900 sec/mm², diffusion time=25ms. Each MRI was reviewed by a pediatric radiologist to evaluate for placental malformations.

Imaging: Post-processing

Manual delineation of the region of interest (ROI) for the entire placenta was created on the b value of 25sec/mm² of the PGSE sequence, using ITK-SNAP. The corresponding T2

weighted image was used as anatomical reference (Figure 1) using the amniotic space as the fetal boundary and the internal uterine wall as the maternal boundary. The diffusion weighted signals were averaged over the entire ROI and IVIM parameters were calculated from the averaged signals.

Motion correction between volumes was performed using the image registration toolkit (IRTK) (26). We then performed an intravoxel-incoherent motion (IVIM) analysis to measure the diffusion coefficient (D , estimate of small scale diffusion), pseudo-diffusion coefficient (D^* , estimate of large scale diffusion) and the perfusion fraction (f , percent of moving blood volume).

Sonography

All pregnancies complicated by FGR underwent complete fetal sonographic assessment of both anatomy and Doppler evaluation as part of the study protocol on the same day as the MRI study using a LOGIQ E9 ultrasound scanner (GE Healthcare, WI). Abdominal circumference, head circumference, femur length and estimated fetal weight were measured and plotted according to gestational age GA (15). Fetal middle cerebral (MCA) and umbilical arterial (UA) flow velocities were measured using a pulse-wave Doppler, and pulsatility indices (PI) were calculated. The cerebroplacental ratio (CPR) was calculated by dividing the middle cerebral artery pulsatility index by the umbilical artery pulsatility index (27). Subjects were classified into the sub-group of abnormal Doppler studies if the CPR was less than 1 (28). All sonographic studies were reviewed by a single attending radiologist as per institutional protocol.

Healthy control pregnancies underwent complete fetal echocardiographic assessment using a Vivid 7 ultrasound scanner (GE Healthcare, Waukesha, WI) as part of an adjunct prospective study. Fetal middle cerebral and umbilical arterial flow velocities were measured using a pulse-wave Doppler; pulsatility indices, CPR and z-scores (derived from normal references) were calculated (28).

Clinical data

Clinical and demographic data were extracted from the maternal and neonatal charts, including race, ethnicity, maternal co-morbidities, fetal sex, and gestational age at study. Neonatal outcomes included gestational age and birthweight at delivery. Available placental pathology reports were also extracted from the medical record, and scored as normal or abnormal, based on pathology report.

Biostatistics

Group comparisons between FGR and controls were evaluated by independent samples t-test or independent chi-square as appropriate. Linear and non-linear associations between IVIM measures and GA at study, maternal age, birth weight and GA at birth, alone and by fetal sex, were evaluated using generalized linear regression; quadratic terms were included in models to evaluate non-linear associations. Additional adjustments for potential co-morbidities were evaluated and subsequently accounted for in diffusion and perfusion fraction analyses, including maternal age, fetal gender and GA at MRI, using ANCOVA.

Least squares means estimates were used for pairwise comparisons. Categorical outcomes for normal-abnormal placental pathology reports within FGR cases were analyzed via independent samples t-test. Associations with neonatal outcomes were also investigated. SAS 9.4 software was used for all analyses (29); a two-tailed p-value of 0.05 was considered significant.

Results

Subjects

We studied 137 pregnant women, 101 recruited as normal controls and 36 with FGR. In the control group, 94 women delivered term, appropriate for gestational age (AGA) infants, 3 (2.97%) delivered preterm, and 4(3.96%) delivered small for gestational age (SGA) infants, with birth weights < 10th centile. Only the 94 healthy women with term, AGA infants were included for the group analyses between controls and FGR cases in order to compare FGR to true healthy controls, while the full cohort of 101 healthy recruits were included in the neonatal outcomes analysis to fully evaluate associations with placental diffusion. Women diagnosed with FGR were further categorized into (1) early onset and late onset (diagnosed in second vs. third trimester), (2) those with or without abnormal Doppler studies of the fetal circulation (namely, CPR < or > 1), and (3) significant maternal comorbidities. Five FGR cases (14%) were noted to have maternal hypertensive disorders (chronic hypertension, gestational hypertension and preeclampsia) and there were no cases of FGR with maternal diabetes mellitus or autoimmune disorders. Of the five FGR cases with maternal hypertensive disorders, 3 also had a CPR <1.0 at the time of evaluation. Approximately one-third (31%) of pregnancies were diagnosed early (in the second trimester) while the remainder were diagnosed in the third trimester and 41.6% of FGR cases overall had abnormal Doppler studies. Additional clinical characteristics are noted in Table 1.

Small-scale water diffusion (D) comparisons in healthy versus FGR pregnancies

Average small-scale water diffusion among healthy controls with normal birth outcomes was $1.76 \times 10^{-3} \text{ mm}^2/\text{s}$, with a negative association between D and advancing gestational age ($\beta = -0.01$, $p=0.06$) (Supplementary Figure 1). While there was no significant difference in D between controls and FGR cases overall, there was a significant *increase* in D in late-onset FGR compared to controls and to early-onset FGR (Table 2). D was associated with pregnancy outcome diffusion was associated with gestational age at birth (non-linear association, $p=0.05$ Figure 2)..

Large-scale water pseudo-diffusion (D*) comparisons in healthy versus FGR pregnancies

Average D* among healthy controls with normal birth outcomes was $36.80 \times 10^{-3} \text{ mm}^2/\text{s}$, with no significant association between D* and advancing gestational age). There was no significant difference in D* between controls and FGR cases overall,, however D* was greater in late-onset FGR compared to controls (Table 2).

D* was associated with pregnancy outcome with a similar non-linear association with gestation age at birth ($p=0.05$ Figure 3) as well as birth weight ($p=0.15$).

Perfusion Fraction, f

The average perfusion fraction among healthy controls with normal birth outcomes was 40.65%. Overall, pregnancies complicated by FGR had lower perfusion fraction compared to controls, even when accounting for GA at the time of evaluation ($p=0.19$) (Table 2). Interestingly, late-onset FGR had the lowest perfusion fraction when compared to controls or early-onset FGR (Table 2). We did not detect any association with placental perfusion fraction and pregnancy outcomes, namely gestational age at birth weight, or birth weight.

IVIM measures and placental pathology in FGR pregnancies

Placental pathology reports were available in the medical records for 22 subjects with FGR (61%). Eighty-two percent of the placentas were noted to weigh less than the 3rd centile for gestational age (30) and 68% had noted abnormalities in thrombi, fibrin deposition, inflammatory changes and accelerated villous maturation. However, there were no significant associations between IVIM measures of D, D* and f and pathology findings ($p = 0.59-0.80$).

Discussion

Principal Findings

Despite several formative studies describing placental perfusion in the human pregnancy through DWI, the microstructural properties of the *in vivo* placenta remain poorly understood (10, 11, 31–35). In this work, we use DWI to report on microstructural development of the *in vivo* human placenta in a large cohort of healthy women with normal pregnancy outcomes, as well as pregnancies complicated by FGR. We show placental diffusion, pseudodiffusion and perfusion fraction are significantly different in late-onset FGR, which has not been previously reported. There were no significant differences in placental microstructure for pregnancies complicated by FGR with a CPR <1, though D, D* and f trended lower in this group. Similarly, pregnancies complicated by FGR with maternal hypertensive disorders trended lower in D and D*, with similar f, although again, these did not achieve statistical significance.

Principles of Diffusion Weighted Imaging and Placental Interpretations

Diffusion of water molecules in biologic tissues is primarily constrained by cell membranes and macromolecules (8). In biomedical imaging, decreased small-scale diffusion is largely interpreted to indicate increased cellular density or regional fibrosis (36), while large-scale pseudo-diffusion represents the diffusion of water molecules in blood, or the microcirculation (36). It is important to note that the application and interpretation of IVIM in the placenta has not been fully delineated or validated with *ex vivo* pathology. However, extending these basic principles of DWI and IVIM suggests that in the placenta, water movement would be most constrained within the highly cellular villi, and least constrained within the open intervillous space. Similarly, it is also worthwhile to note that there is likely significant correlation between pseudo-diffusion (D*) and the moving blood fraction (f) given the relatively open areas of the intervillous space. However, despite these limitations,

the *in vivo* findings of this study coupled with known pathological changes in placental insufficiency are in line with these interpretations.

Lessons from Placental Histopathology & Clinical Outcomes

Characterizing placental pathology has been challenging due to both variability in clinical and histopathologic definitions, as well as the wide variety of lesions described within a single clinical entity (37, 38). The pathology of late-onset FGR is not as well understood as other forms of FGR. Histologically, placental changes are much more variable and often time, unremarkable in late-onset FGR (39). If placental changes are noted, there is an increased incidence of vascular lesions, including infarction. In this study, late-onset FGR was significantly associated with increased small-scale and large-scale water diffusion of the placenta. In addition, late-onset FGR had the most significant reduction in f , or the percent of moving blood, which may result from such vascular lesions. However, further studies are needed to better understand the pathologic changes in the placenta of late-onset FGR and the relationship with these *in vivo* DWI findings.

Conversely, maternal vascular underperfusion, common in preeclampsia-eclampsia and FGR, is characterized by placental hypoplasia grossly, and by villous hypoplasia and accelerated villous maturation histologically (40–42). Conversely, there are reports of *increased* placental weight associated with decreased distal villous hypoplasia in preeclampsia (43). Likewise, villous hypoplasia has been described in both early-onset FGR and pregnancies with abnormalities of umbilical artery resistance, as seen with reduced CPR (39, 44). Interestingly, there is one report of 5 cases of maternal vascular underperfusion and retrospective analysis of placental DWI that revealed reduced diffusion compared to placental diffusion in normal pregnancies (45). Similarly, our data suggests reduced small-scale diffusion through IVIM analysis in our cohort of FGR cases with maternal hypertensive disorders, including preeclampsia. There is a similar suggestion of decreased small-scale diffusion in early-onset FGR and FGR cases with decreased CPR.

While the cellular mechanisms that may explain these findings are unclear, our data suggests that IVIM may provide insight into *in vivo* microstructural and microvascular development. Furthermore, there appears to be an optimal range of diffusion and pseudo-diffusion parameters, as measure by IVIM analyses, associated with birth outcomes, including term birth with normal birth weights.

Strengths and Limitations

In this work, we show that DWI can detect important differences in the placenta of growth-restricted pregnancies when compared to healthy controls, particularly in late-onset FGR, with notable trends in FGR with decreased CPR or FGR with MHD. Despite the many strengths of this work, there are important limitations that deserve mention. First, while IVIM analysis can distinguish differential diffusion properties across tissue classes, it is highly dependent on the number and range of b values acquired (9). While our MRI acquisition protocol was sensitive enough to detect important differences in healthy and high-risk pregnancies, the optimal sequences, correction methods and analysis models for placental diffusion remain to be determined (46). Secondly, the objective of this study was to

characterize placental diffusion and perfusion in high-risk pregnancies with established FGR.

However, as discussed throughout the manuscript, there are multiple pathologic pathways that can converge to result in fetal growth anomalies. While our data suggests that IVIM may be able to distinguish between early- and late-onset FGR, some of the sub-group analyses were limited by the smaller sample sizes – particularly pregnancies complicated by FGR with MHD. Nonetheless, these data present intriguing trends that should be further studied in larger cohorts of individual high-risk conditions. Similarly, we were unable to identify any significant relationships between *in vivo* placental development and *ex vivo* histopathology. The temporal evolution of placental development and disease from the point of imaging to the point of delivery and pathology evaluation may have confounded our findings. However, these analyses were further limited by the retrospective data collection of the pathology reports. Nonetheless, relating these findings prospectively with planned placental pathology evaluations is needed to validate these findings, as well as the proposed interpretations. Lastly, while we were able to identify important relationships between *in vivo* placental water diffusion and birth outcomes, the predictive validity and clinical relevance of these findings require confirmation in larger cohorts and with long-term neurodevelopmental outcome. These studies are currently underway.

Conclusions

While advances in prenatal care have improved pregnancy outcomes and fetal mortality, there remain significant limitations in identifying early and sensitive biomarkers of placental health (47–49). In this work, we proposed that *in vivo* placental microstructure can be assessed with diffusion weighted imaging, and identify potential markers of aberrant placental development in high-risk pregnancies. Once mechanisms of placental growth and function become better established, future screening, surveillance and treatment can be tailored to individual maternal-fetal dyads and improve short- and long-term pregnancy outcomes.

Supplementary Material

Refer to Web version on PubMed Central for supplementary material.

Acknowledgements:

This work has been supported by National Institutes of Health (R01-HL116585, 1U54HD090257, UL1TR000075, KL2TR000076, 1K23HD092585).

Funding sources: Supported by National Institutes of Health (R01-HL116585, 1U54HD090257, UL1TR000075, KL2TR000076, 1K23HD092585–01A1).

Abbreviations

FGR	fetal growth restriction
MRI	magnetic resonance imaging
DWI	diffusion weighted imaging

IVIM	intra-voxel incoherent motion analysis
D	diffusion coefficient
D*	pseudo-diffusion coefficient
f	perfusion fraction

References:

- Bernstein IM, Horbar JD, Badger GJ, Ohlsson A, Golan A. Morbidity and mortality among very-low-birth-weight neonates with intrauterine growth restriction. The Vermont Oxford Network. *Am J Obstet Gynecol.* 2000;182(1 Pt 1):198–206. [PubMed: 10649179]
- Joss-Moore LA, Lane RH. The developmental origins of adult disease. *Curr Opin Pediatr.* 2009;21(2):230–4. [PubMed: 19663040]
- Baschat AA. Neurodevelopment following fetal growth restriction and its relationship with antepartum parameters of placental dysfunction. *Ultrasound Obstet Gynecol.* 2011;37(5):501–14. [PubMed: 21520312]
- Heazell AE, Whitworth M, Duley L, Thornton JG. Use of biochemical tests of placental function for improving pregnancy outcome. *The Cochrane database of systematic reviews.* 2015(11):CD011202.
- Baschat AA. Planning management and delivery of the growth-restricted fetus. *Best practice & research Clinical obstetrics & gynaecology.* 2018;49:53–65. [PubMed: 29606482]
- Levytska K, Higgins M, Keating S, Melamed N, Walker M, Sebire NJ, et al. Placental Pathology in Relation to Uterine Artery Doppler Findings in Pregnancies with Severe Intrauterine Growth Restriction and Abnormal Umbilical Artery Doppler Changes. *Am J Perinatol.* 2017;34(5):451–7. [PubMed: 27649292]
- Parra-Saavedra M, Crovetto F, Triunfo S, Savchev S, Peguero A, Nadal A, et al. Placental findings in late-onset SGA births without Doppler signs of placental insufficiency. *Placenta.* 2013;34(12):1136–41. [PubMed: 24138874]
- Iima M, Le Bihan D. Clinical Intravoxel Incoherent Motion and Diffusion MR Imaging: Past, Present, and Future. *Radiology.* 2016;278(1):13–32. [PubMed: 26690990]
- Le Bihan D. What can we see with IVIM MRI? *NeuroImage* 2017.
- Sohlberg S, Mulic-Lutvica A, Lindgren P, Ortiz-Nieto F, Wikstrom AK, Wikstrom J. Placental perfusion in normal pregnancy and early and late preeclampsia: a magnetic resonance imaging study. *Placenta.* 2014;35(3):202–6. [PubMed: 24529946]
- Moore RJ, Strachan BK, Tyler DJ, Duncan KR, Baker PN, Worthington BS, et al. In utero perfusing fraction maps in normal and growth restricted pregnancy measured using IVIM echo-planar MRI. *Placenta.* 2000;21(7):726–32. [PubMed: 10985977]
- Moore RJ, Issa B, Tokarczuk P, Duncan KR, Boulby P, Baker PN, et al. In vivo intravoxel incoherent motion measurements in the human placenta using echo-planar imaging at 0.5 T. *Magn Reson Med.* 2000;43(2):295–302. [PubMed: 10680695]
- Veerbeek JH, Nikkels PG, Torrance HL, Gravesteyn J, Post Uiterweer ED, Derks JB, et al. Placental pathology in early intrauterine growth restriction associated with maternal hypertension. *Placenta.* 2014;35(9):696–701. [PubMed: 25052232]
- Aviram A, Sherman C, Kingdom J, Zaltz A, Barrett J, Melamed N. Defining early vs late fetal growth restriction by placental pathology. *Acta Obstet Gynecol Scand.* 2019;98(3):365–73. [PubMed: 30372519]
- Hadlock FP, Deter RL, Harrist RB, Park SK. Estimating fetal age: computer-assisted analysis of multiple fetal growth parameters. *Radiology.* 1984;152(2):497–501. [PubMed: 6739822]
- Tustison NJ, Avants BB, Cook PA, Zheng Y, Egan A, Yushkevich PA, et al. N4ITK: improved N3 bias correction. *IEEE Trans Med Imaging.* 2010;29(6):1310–20. [PubMed: 20378467]
- Coupe P, Yger P, Prima S, Hellier P, Kervrann C, Barillot C. An optimized blockwise nonlocal means denoising filter for 3-D magnetic resonance images. *IEEE Trans Med Imaging.* 2008;27(4):425–41. [PubMed: 18390341]

18. Erturk MA, Bottomley PA, El-Sharkawy AM. Denoising MRI using spectral subtraction. *IEEE Trans Biomed Eng.* 2013;60(6):1556–62. [PubMed: 23322757]
19. Ferrazzi G, Kuklisova Murgasova M, Arichi T, Malamateniou C, Fox MJ, Makropoulos A, et al. Resting State fMRI in the moving fetus: a robust framework for motion, bias field and spin history correction. *Neuroimage.* 2014;101:555–68. [PubMed: 25008959]
20. Gholipour A, Estroff JA, Warfield SK. Robust super-resolution volume reconstruction from slice acquisitions: application to fetal brain MRI. *IEEE Trans Med Imaging.* 2010;29(10):1739–58. [PubMed: 20529730]
21. Holtrop JL, Sutton BP. High spatial resolution diffusion weighted imaging on clinical 3 T MRI scanners using multislab spiral acquisitions. *J Med Imaging (Bellingham).* 2016;3(2):023501.
22. Kim K, Habas PA, Rousseau F, Glenn OA, Barkovich AJ, Studholme C. Intersection based motion correction of multislice MRI for 3-D in utero fetal brain image formation. *IEEE Trans Med Imaging.* 2010;29(1):146–58. [PubMed: 19744911]
23. Rousseau F, Glenn OA, Iordanova B, Rodriguez-Carranza C, Vigneron DB, Barkovich JA, et al. Registration-based approach for reconstruction of high-resolution in utero fetal MR brain images. *Acad Radiol.* 2006;13(9):1072–81. [PubMed: 16935719]
24. Rousseau F, Oubel E, Pontabry J, Schweitzer M, Studholme C, Koob M, et al. BTK: an opensource toolkit for fetal brain MR image processing. *Comput Methods Programs Biomed.* 2013;109(1):65–73. [PubMed: 23036854]
25. Seshamani S, Cheng X, Fogtmann M, Thomason ME, Studholme C. A method for handling intensity inhomogenities in fMRI sequences of moving anatomy of the early developing brain. *Med Image Anal.* 2014;18(2):285–300. [PubMed: 24317121]
26. You W, Serag A, Evangelou IE, Andescavage N, Limperopoulos C. Robust motion correction and outlier rejection of in vivo functional MR images of the fetal brain and placenta during maternal hyperoxia. *Proc SPIE Int Soc Opt Eng.* 2015;9417:941700.
27. Ebbing C, Rasmussen S, Kiserud T. Middle cerebral artery blood flow velocities and pulsatility index and the cerebroplacental pulsatility ratio: longitudinal reference ranges and terms for serial measurements. *Ultrasound Obstet Gynecol.* 2007;30(3):287–96. [PubMed: 17721916]
28. Baschat AA, Gembruch U. The cerebroplacental Doppler ratio revisited. *Ultrasound Obstet Gynecol.* 2003;21(2):124–7. [PubMed: 12601831]
29. SAS. SAS system. 9.3 ed. Cary, NC.: SAS Institute Inc; 7 2011.
30. Almog B, Shehata F, Aljabri S, Levin I, Shalom-Paz E, Shrim A. Placenta weight percentile curves for singleton and twins deliveries. *Placenta.* 2011;32(1):58–62. [PubMed: 21036395]
31. Bonel HM, Stolz B, Diedrichsen L, Frei K, Saar B, Tutschek B, et al. Diffusion-weighted MR imaging of the placenta in fetuses with placental insufficiency. *Radiology.* 2010;257(3):810–9. [PubMed: 21084415]
32. Derwig I, Lythgoe DJ, Barker GJ, Poon L, Gowland P, Yeung R, et al. Association of placental perfusion, as assessed by magnetic resonance imaging and uterine artery Doppler ultrasound, and its relationship to pregnancy outcome. *Placenta.* 2013;34(10):885–91. [PubMed: 23937958]
33. Siauve N, Hayot PH, Deloison B, Chalouhi GE, Alison M, Balvay D, et al. Assessment of human placental perfusion by intravoxel incoherent motion MR imaging. *J Matern Fetal Neonatal Med.* 2017:1–8.
34. Sohlberg S, Mulic-Lutvica A, Olovsson M, Weis J, Axelsson O, Wikstrom J, et al. Magnetic resonance imaging-estimated placental perfusion in fetal growth assessment. *Ultrasound Obstet Gynecol.* 2015;46(6):700–5. [PubMed: 25640054]
35. Jakab A, Tuura RL, Kottke R, Ochsenbein-Kolble N, Natalucci G, Nguyen TD, et al. Microvascular perfusion of the placenta, developing fetal liver, and lungs assessed with intravoxel incoherent motion imaging. *J Magn Reson Imaging.* 2018;48(1):214–25. [PubMed: 29281153]
36. Mannelli L, Nougaret S, Vargas HA, Do RK. Advances in diffusion-weighted imaging. *Radiol Clin North Am.* 2015;53(3):569–81. [PubMed: 25953290]
37. Redline RW. Thrombophilia and placental pathology. *Clinical obstetrics and gynecology.* 2006;49(4):885–94. [PubMed: 17082683]
38. Redline RW. Placental pathology: a systematic approach with clinical correlations. *Placenta.* 2008;29 Suppl A:S86–91. [PubMed: 17950457]

39. Mifsud W, Sebire NJ. Placental pathology in early-onset and late-onset fetal growth restriction. *Fetal Diagn Ther.* 2014;36(2):117–28. [PubMed: 24577279]
40. Khong TY, Mooney EE, Ariel I, Balmus NC, Boyd TK, Brundler MA, et al. Sampling and Definitions of Placental Lesions: Amsterdam Placental Workshop Group Consensus Statement. *Arch Pathol Lab Med.* 2016;140(7):698–713. [PubMed: 27223167]
41. Redline RW, Boyd T, Campbell V, Hyde S, Kaplan C, Khong TY, et al. Maternal vascular underperfusion: nosology and reproducibility of placental reaction patterns. *Pediatr Dev Pathol.* 2004;7(3):237–49. [PubMed: 15022063]
42. Ernst LM. Maternal vascular malperfusion of the placental bed. *APMIS.* 2018;126(7):551–60. [PubMed: 30129127]
43. Stark MW, Clark L, Craver RD. Histologic differences in placentas of preeclamptic/eclamptic gestations by birthweight, placental weight, and time of onset. *Pediatr Dev Pathol.* 2014;17(3):181–9. [PubMed: 24625285]
44. Kingdom J, Huppertz B, Seaward G, Kaufmann P. Development of the placental villous tree and its consequences for fetal growth. *European journal of obstetrics, gynecology, and reproductive biology.* 2000;92(1):35–43.
45. Haals HDN, Sinding M, Peters D, Petersen A, Frokjaer JB, Overgaard C, Sorensen A. Diffusion-weighted MRI of the placenta in normal pregnancies and in pregnancies complicated by fetal growth restriction. *Ultrasound Obstet Gynecol.* 2016;48(S1):145.
46. Slator PJ, Hutter J, McCabe L, Gomes ADS, Price AN, Panagiotaki E, et al. Placenta microstructure and microcirculation imaging with diffusion MRI. *Magn Reson Med.* 2018;80(2):756–66. [PubMed: 29230859]
47. Alfirevic Z, Stampalija T, Dowswell T. Fetal and umbilical Doppler ultrasound in high-risk pregnancies. *The Cochrane database of systematic reviews.* 2017;6:CD007529.
48. Baschat AA, Gembruch U, Weiner CP, Harman CR. Qualitative venous Doppler waveform analysis improves prediction of critical perinatal outcomes in premature growth-restricted fetuses. *Ultrasound Obstet Gynecol.* 2003;22(3):240–5. [PubMed: 12942494]
49. Goffinet F, Paris-Llado J, Nisand I, Breart G. Umbilical artery Doppler velocimetry in unselected and low risk pregnancies: a review of randomised controlled trials. *Br J Obstet Gynaecol.* 1997;104(4):425–30. [PubMed: 9141578]

- Placental dysfunction can impact both maternal and fetal well-being
- Histologic changes in placental development have been described in fetal growth restriction
- Microstructural changes of the placenta remain difficult to identify *in vivo*
- Diffusion weighted magnetic resonance imaging is used to described *in vivo* microstructure
- Small scale diffusion and the perfusion fraction of the *in vivo* placenta is reduced in fetal growth restriction

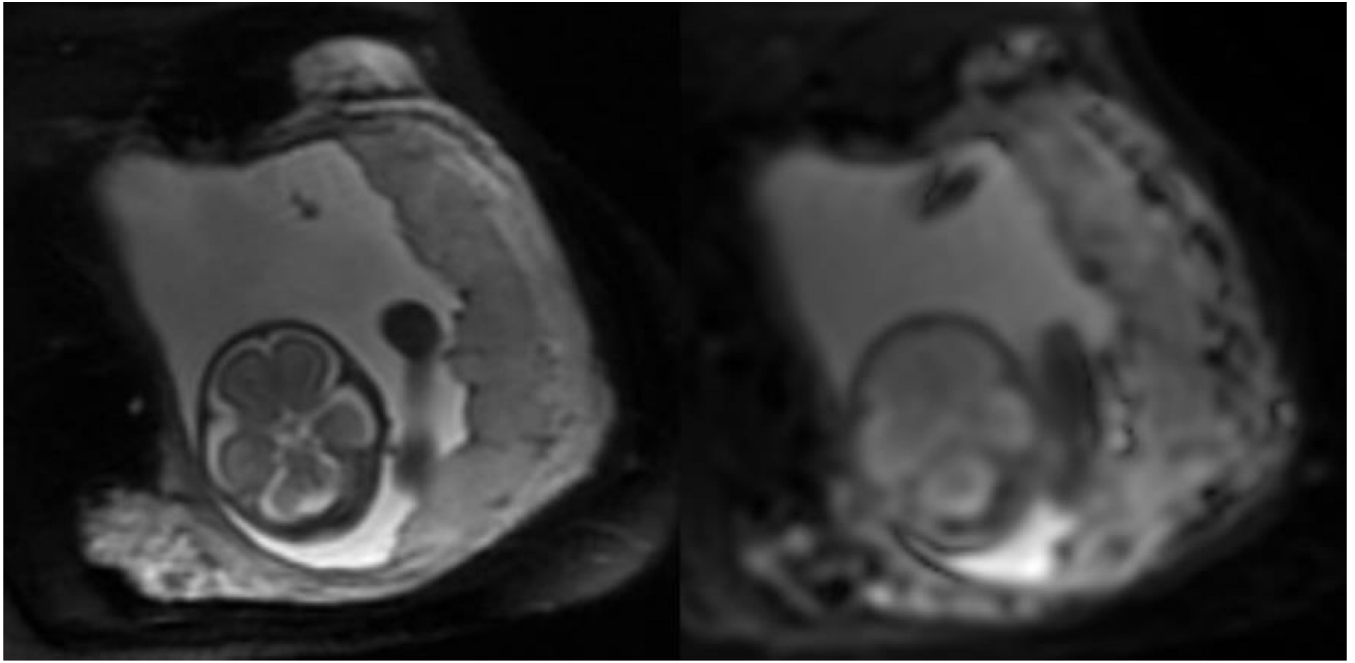


Figure 1:
Example of magnetic resonance images (MRI), including the T2Weighted anatomic image of the placenta (A), and the corresponding Diffusion weighted image (DWI) (b0 acquisition) (B) at 25 weeks gestation.

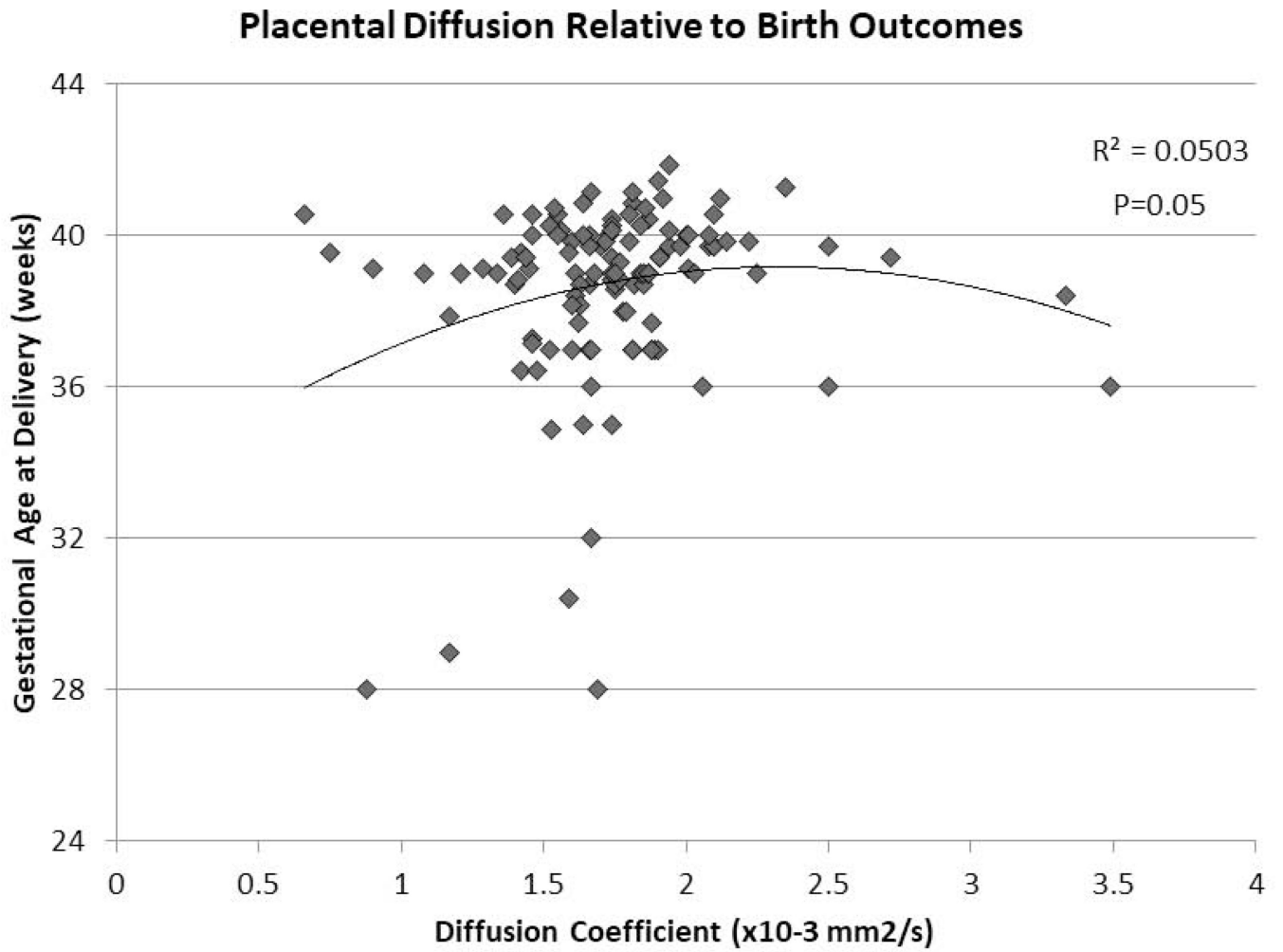


Figure 2:
The diffusion coefficient (D) of the *in vivo* placenta through IVIM analyses of DWI and pregnancy outcomes; namely gestational age at birth.

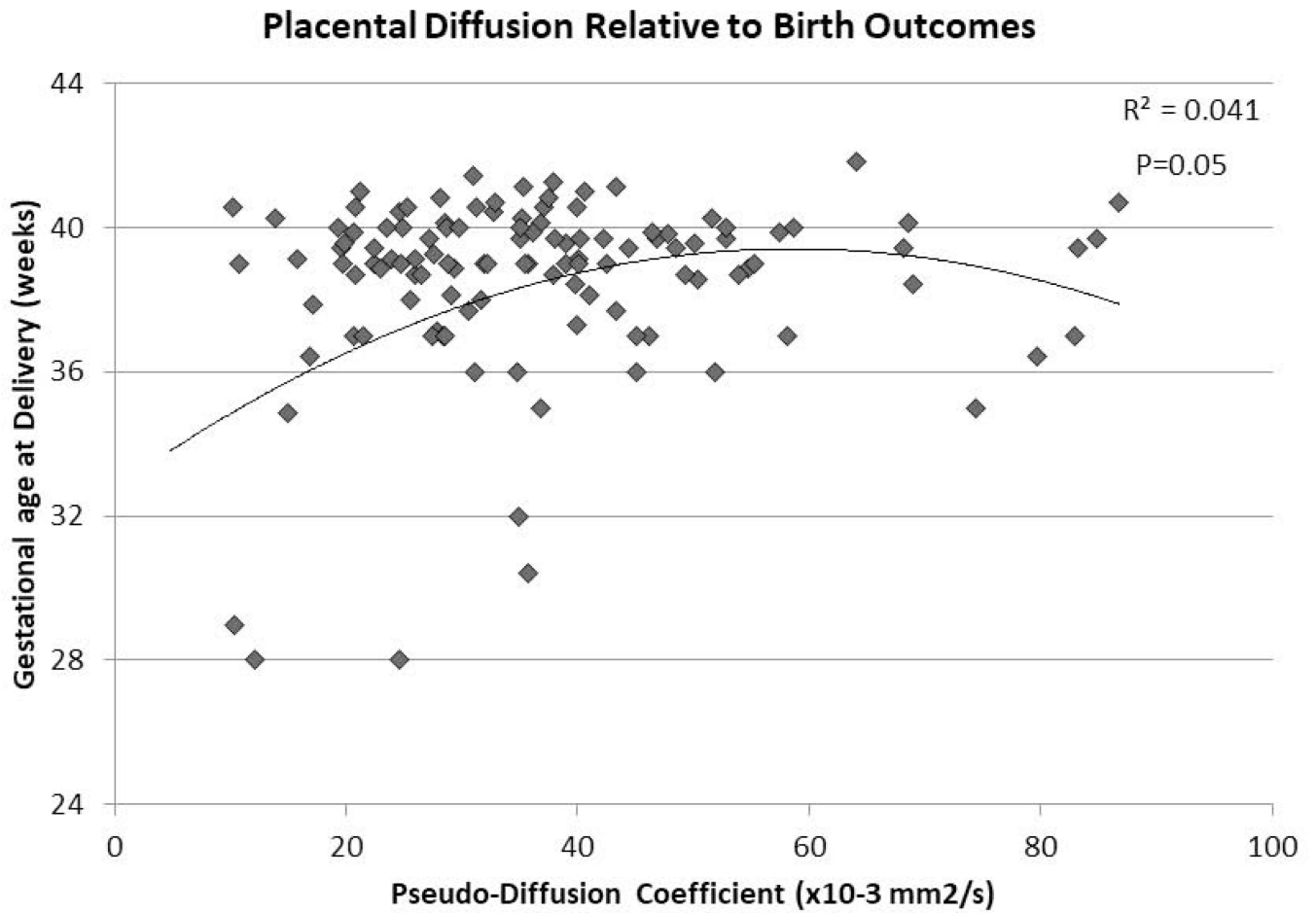


Figure 3:
The pseudo-diffusion coefficient (D^*) of the *in vivo* placenta through IVIM analyses of DWI and pregnancy outcome; namely gestational age at.

Clinical Characteristics

Table 1:

	Healthy Control (n=101)	Fetal Growth Restriction (n=36)	P-value
Maternal Age (years)	29.9 ± 6.9	24.7 ± 6.2	0.10
Gestational Age at MRI (weeks)	29.1 ± 5.8	31.0 ± 3.8	0.07
Fetal Gender, Male (n, %)	52 (51.5%)	13 (36.1%)	0.17
Neonatal Data			
Gestational Age at birth (weeks)	39.35 ± 1.55	36.91 ± 3.19	0.0001
Birth weight (grams)	3288 ± 438	2312 ± 663	0.0001
Birth weight (z-score)	-0.18 ± 0.77	-1.52 ± 0.73	0.0001

Table 2.

Placental diffusion metrics across healthy and high-risk pregnancies

	Control (n=97)	FGR (n=36)	p-value ^a
Small Scale Diffusion (D)	1.76	1.74	0.76
Large Scale Pseudo-Diffusion (D*)	36.80	34.14	0.42
Perfusion Fraction (f, %)	40.65	37.68	0.19
	Control (n=97)	Early-Onset FGR (n=11)	Late-Onset FGR (n=25)
Small Scale Diffusion (D)	1.76	1.50	1.87 ^{c, d}
Large Scale Pseudo-Diffusion (D*)	36.80	23.56	39.42 ^d
Perfusion Fraction (f, %)	40.65	45.94	34.13 ^{c, d}
	Control (n=97)	FGR, CPR >1 (n=21)	FGR, CPR <1 (n=15)
Small Scale Diffusion (D)	1.76	1.82	1.66
Large Scale Pseudo-Diffusion (D*)	36.80	37.51	29.23
Perfusion Fraction (f, %)	40.65	37.60	38.51
	Control (n=97)	FGR, No MHD (n=31)	FGR, + MHD (n=05)
Small Scale Diffusion (D)	1.76	1.79	1.50
Large Scale Pseudo-Diffusion (D*)	36.80	35.60	23.07
Perfusion Fraction (f, %)	40.65	37.33	41.90

^aBased on independent samples t-test^bPairwise comparisons based on least squares means estimates from ANOVA^csignificantly different from control at p < 0.05^dsignificantly different from early-onset FGR at p < 0.05

Abbreviations: FGR=fetal growth restriction, CPR=cerebroplacental ratio, MHD=maternal hypertensive disorders (namely, gestational hypertension, chronic hypertension and preeclampsia)